

Synthesis, antiproliferative activity and autophagic flux inhibition of new arylsparteine derivatives



Moustafa T. Gabr^{a,b,*}, Mohammed S. Abdel-Raziq^{c,d}

^a Department of Medicinal Chemistry, Faculty of Pharmacy, Mansoura University, Mansoura 35516, Egypt

^b Department of Chemistry, University of Iowa, Iowa City, Iowa, 52242, United States

^c Department of Pharmacognosy, Faculty of Pharmacy, Mansoura University, Mansoura, 35516, Egypt

^d School of Chemistry and Molecular Biosciences, University of Queensland, St Lucia, 4072, Queensland, Australia

ARTICLE INFO

Keywords:

Sparteine
Autophagic flux
Antiproliferative activity
Autophagy inhibition
Quinolizidine alkaloids

ABSTRACT

New series of arylsparteine derivatives were synthesized and evaluated for their cytotoxic activity against four human cancer cell lines (cervical epithelial carcinoma cells Hela, breast cancer cells MCF-7, lung cancer cells A549, and glioma cells U87 MG) and one normal fibroblast cell line. Structure-activity relationship revealed that introduction of 4-quinolinylnyl moiety to sparteine afforded a hybrid compound **10** with considerable antiproliferative activity against all tested cancer cell lines. Compound **10**, the most active agent in this study possessed IC₅₀ values of 5.97 ± 1.1 and 9.52 ± 0.3 μM against A549 and Hela cancer cell lines, respectively. Inhibition of autophagic flux proved to be the underlying mechanism for the antiproliferative activity of **10** which was further validated by decreased levels of ATP in cancer cells treated with **10**. In addition, co-treatment of **10** and rapamycin restored cell viability which comes in good agreement with the proposed autophagic flux inhibition for **10**.

1. Introduction

Natural products and their derivatives are valuable leads for the development of cancer therapeutics (Khazir et al., 2014). Quinolizidine alkaloids have demonstrated promising activity against non-small cell lung carcinoma, liver cancer and gastric cancer (Bao et al., 2014; Guo et al., 2015; Xu et al., 2011; Yang et al., 2013; Zhao et al., 2014). In this context, sophoridine (**1**, Fig. 1), a quinolizidine natural product, emerged as a promising chemical entity for drug development owing to its structural flexibility and favorable pharmacokinetic profile (Wei et al., 2006). In addition, **1** exhibits considerable cytotoxic activity which is attributed to the induction of apoptosis and the cell cycle arrest at the S-phase (Xu et al., 2017). Matrine (**2**, Fig. 1), extracted from *Sophora flavescens* Ait, was approved by Chinese FDA as an antiproliferative drug for non-small cell lung cancer and liver cancer (Sun et al., 2012). Consequently, tremendous research efforts have been directed towards development of sophoridine and matrine derivatives as potential antiproliferative agents (Bi et al., 2014, 2016; Wang et al., 2012; Zhao et al., 2015). Sparteine (**3**, Fig. 1), a quinolizidine alkaloid, is known to be a principal constituent of *Lupinus mutabilis* (Hatzold et al., 1983). The biological activities of sparteine as an antiarrhythmic (Pugsley et al., 1995) and hypoglycemic agents (Garcia-Lopez et al.,

2004) have been widely studied. However, development of sparteine derivatives with potential antiproliferative activity remains unexplored.

Autophagy is a cellular degradation pathway for the clearance of undesired cellular components via lysosomal degradation. Autophagic pathway sustains metabolic pathways required for survival of different cancer types. (Anding and Baehrecke, 2015; Galluzzi et al., 2014). Quinoline-based compounds have displayed the ability to accumulate in acidic lysosomes of cancer cells resulting in disruption of autophagy (Amaravadi et al., 2007; Carew et al., 2007; Golden et al., 2015). Chloroquine (CQ), the prototypical antimalarial drug, received considerable attention as a potential antiproliferative agent because of its ability to block autophagic flux. However, severe side effects of CQ including ocular toxicity developed a pressing need for identification of new inhibitors of autophagy (Wang et al., 2017). Recently, sophoridine derivatives emerged as novel autophagy inhibitors owing to their lysosomotropic property similarly to CQ (Bi et al., 2017). Taking all these findings into consideration, new arylsparteine derivatives were synthesized and evaluated for their antiproliferative activity against four human cancer cell lines (cervical epithelial carcinoma cells Hela, breast cancer cells MCF-7, lung cancer cells A549, and glioma cells U87 MG) and one normal fibroblast cell line. Moreover, the ability of the new arylsparteine derivatives to block autophagic flux is investigated.

* Corresponding author.

E-mail address: gabr2003@gmail.com (M.T. Gabr).

<https://doi.org/10.1016/j.phytol.2018.07.022>

Received 6 May 2018; Received in revised form 13 June 2018; Accepted 13 July 2018

1874-3900/ © 2018 Phytochemical Society of Europe. Published by Elsevier Ltd. All rights reserved.

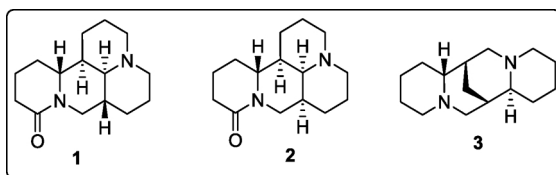


Fig. 1. Chemical structures of 1-3.

2. Results and discussion

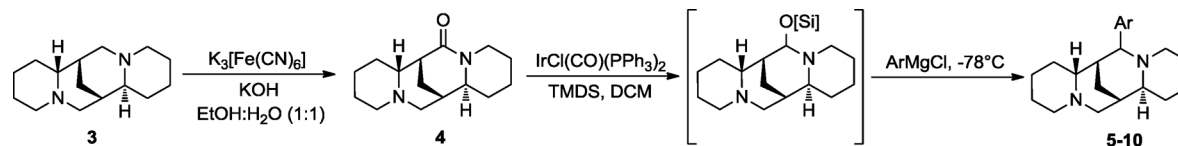
A general approach for the synthesis of the target compounds is outlined in Scheme 1. 17-Oxosparteine **4** was obtained through oxidation of the parent sparteine **3** through a modification of previously described procedure (Golebiewski and Spenser, 1985). In addition, a two-stage iridium catalyzed reductive coupling of **4** and Grignard reagents furnished arylsparteine derivatives **5–10** in serviceable yields. All target compounds were characterized by HRMS, ^1H NMR, and ^{13}C NMR. The cytotoxic activity of **5–10** against four human cancer cell lines (cervical epithelial carcinoma cells Hela, breast cancer cells MCF-7, lung cancer cells A549, and glioma cells U87 MG) and one normal cell line (mouse embryo fibroblasts NIH3T3) was evaluated using MTT assay. The IC_{50} values of the target compounds **5–10**, sparteine, and the reference drug 5-fluorouracil are listed in Table 1. The parent sparteine **3** displayed negligible cytotoxicity with IC_{50} values $> 50 \mu\text{M}$ against all tested cell lines. Compound **5** bearing phenyl ring as the aryl substituent displayed minimal improvement in its antiproliferative profile compared to the parent compound **3**. However, compounds **6** and **7** with electron donating groups (EDGs) demonstrated considerable improvement in their potency against tested cancer cell lines. Regarding the substitution pattern on the phenyl ring, 3,4,5-trimethoxy substituted **7** was more active than 4-methoxy-substituted **6**. Compound **7** possessed IC_{50} values of 24.5 ± 1.9 and $28.7 \pm 3.1 \mu\text{M}$ against MCF-7 and A549 cancer cell lines, respectively. Incorporation of methoxy-substituted phenyl rings (EDGs) to quinazolidine alkaloids has been reported to result in considerable improvement in their ability to block the autophagic flux and consequently enhanced antiproliferative activity (Bi et al., 2017). Interestingly, switching to electron withdrawing groups (EWGs) in **8** and **9** further increased the potency of the arylsparteine derivatives against all tested cancer cell lines. In addition, compound **9** bearing 4-nitro-aryl substituent possessed comparable potency to the reference drug 5-fluorouracil against MCF-7 and U87 MG cancer cell lines. We speculate that incorporation of EWGs to arylsparteine derivatives increase their lipophilicity which consequently alter their permeability to cellular membranes resulting in enhanced interaction with cancer cells. A similar trend has been reported for the effect of incorporation of EWGs to quinazolidine alkaloids on their antiproliferative potency (Wang et al., 2012). These results demonstrate

that the substitution pattern of the aryl substituent is a crucial component of the antiproliferative profile of arylsparteine derivatives. Compound **10** bearing 4-quinolinyl moiety as the aryl substituent proved to be the most active member of this study against all tested cancer cell lines. Notably, **10** was more potent than 5-fluorouracil against U87 MG and A549 cell lines with IC_{50} values of 9.71 ± 2.2 and $5.97 \pm 1.1 \mu\text{M}$, respectively. Moreover, **10** displayed potential antiproliferative activity against Hela cell line with IC_{50} value of $9.52 \pm 0.3 \mu\text{M}$ in comparison to IC_{50} value of $8.45 \pm 1.4 \mu\text{M}$ for 5-fluorouracil against the same cell line. It is noteworthy to mention that **10** was less cytotoxic than 5-fluorouracil to the normal NIH3T3 cells with IC_{50} value of $35.1 \pm 2.9 \mu\text{M}$. We speculate that the selectivity of **10** to cancer cells over normal cells in comparison to 5-fluorouracil is attributed to higher sensitivity of cancer cells to autophagy inhibitors based on biochemical and metabolic differences between normal and cancer cells (Galluzzi et al., 2014).

Autophagy in cancer cells results in degradation of long-lived proteins, thus, measuring their rate of degradation is the most frequently used method to monitor the autophagic flux in cancer cells (Dupont et al., 2017). In order to investigate the ability of **10** to block autophagic flux in cancer cells, the effect of **10** on degradation of [^{14}C]-valine-labeled long-lived proteins was evaluated in Hela cancer cells. The results displayed in Fig. 2 reveal that **10** effectively reduce the degradation of long-lived proteins analogously to the autophagy inhibitor, 3-methyladenine (3-MA). Such finding validates the blockade of the autophagic flux in Hela cells by **10**. Low pH value ($\text{pH} < 4.5$) in the lysosome, the central platform for autophagic pathway, is crucial for its proteolytic activity. It is speculated that the basic nitrogen-containing sparteine core is protonated under physiological conditions and further accumulates in lysosomes. Incorporation of the basic 4-quinolinyl moiety contributes to inhibition of lysosomal acidification which prevents subsequent autophagic degradation as previously reported for quinoline-based compounds (Amaravadi et al., 2007; Carew et al., 2007; Golden et al., 2015).

Autophagic flux inhibition decreases the recycling of cellular fuels, which eventually results in reduced levels of adenosine triphosphate (ATP) (Mizushima and Komatsu, 2011). To further demonstrate that compound **10** blocks autophagic flux in cancer cells, the intracellular production of ATP in Hela cells was measured upon treatment with **10**. As shown in Fig. 3, the intracellular ATP level was reduced in the Hela cells treated with **10** (2.5 or $5 \mu\text{M}$) for 48 h. These results come in good agreement with the proposed autophagic blockade mechanism for **10**.

To further validate the proposed mechanism for **10**, the effect of co-treatment of **10** and rapamycin (Rap, autophagy inducer) and CQ (autophagy inhibitor) on cancer cells viability was investigated. Interestingly, co-treatment of **10** ($5 \mu\text{M}$) with Rap ($10 \mu\text{M}$) for 48 h restored U87 MG cells viability as revealed by MTT assay (Fig. 4A). Moreover, compound **10** ($10 \mu\text{M}$) displayed enhanced cytotoxicity with



Comp. No.	Ar	Comp. No.	Ar	Comp. No.	Ar
5		6		7	
8		9		10	

Scheme 1. Synthesis of arylsparteine derivatives **5–10**.

Table 1
Antiproliferative activity (IC₅₀, μM) of compounds 5–10, sparteine and 5-fluorouracil against the tested cell lines.

Comp. No.	IC ₅₀ (μM) ^a > Hela	MCF-7	A549	U87 MG	NIH3T3
5	46.9 ± 3.1	42.9 ± 3.8	> 50	> 50	48.3 ± 1.6
6	38.1 ± 3.4	29.6 ± 2.3	36.4 ± 2.7	41.5 ± 3.8	45.1 ± 1.9
7	30.4 ± 2.9	24.5 ± 1.9	28.7 ± 3.1	33.6 ± 2.6	42.7 ± 1.7
8	25.7 ± 2.6	18.5 ± 1.8	21.3 ± 2.1	24.7 ± 1.4	39.6 ± 2.0
9	21.1 ± 2.2	13.4 ± 1.7	19.7 ± 1.8	16.6 ± 1.9	36.4 ± 1.6
10	9.52 ± 0.3	10.7 ± 1.5	5.97 ± 1.1	9.71 ± 2.2	35.1 ± 2.9
Sparteine	> 50	> 50	> 50	> 50	> 50
5-Fluorouracil	8.45 ± 1.4	10.1 ± 1.2	36.8 ± 3.5	13.4 ± 2.5	19.3 ± 2.1

Bold values point out the best results.

^a Data are shown as SD.

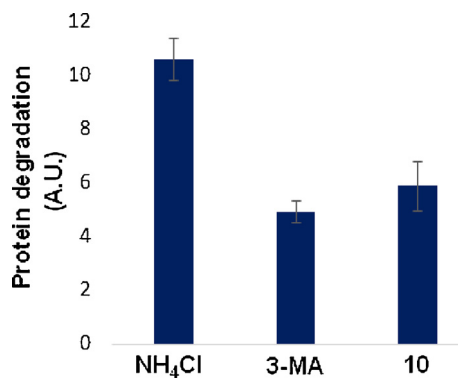


Fig. 2. Assay to measure degradation of long-lived proteins in HeLa cells in the presence of 10 mM of the tested compounds. Bars and error bars represent the mean ± SD in triplicate experiment.

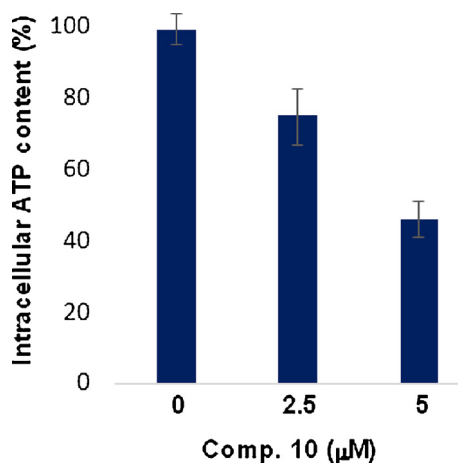


Fig. 3. Intracellular ATP level in HeLa cells treated with compound 10 (10 μM). Bars and error bars represent the mean ± SD in triplicate experiment.

CQ (50 μM) against U87 MG cells in MTT assay after 48 h exposure (Fig. 4B). These results demonstrate that the antiproliferative profile of 10 is directly related to blockade of autophagic flux.

3. Experimental

3.1. Chemistry

All commercially available starting materials, reagents, and solvents were used as supplied, unless otherwise stated. Reported yields are isolated yields. Purification of all final products was accomplished by silica gel flash column chromatography. Proton (¹H) and carbon (¹³C) NMR were collected on Bruker NMR spectrometers at 400 MHz for ¹H and 100 MHz for ¹³C. Chemical shifts (δ) are reported in parts-per

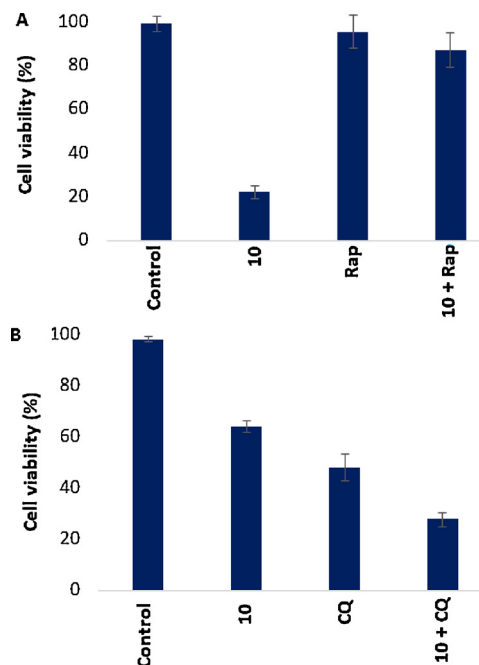


Fig. 4. (A) The effect of co-treatment of 10 (5 μM) and rapamycin (10 μM) on the cell viability of U87 MG cells. (B) The effect of co-treatment of 10 (10 μM) and CQ (50 μM) on the cell viability of U87 MG cells. Bars and error bars represent the mean ± SD in triplicate experiment.

million (ppm) relative to residual undeuterated solvent. Melting points were recorded using a capillary melting point apparatus and are uncorrected. High resolution mass spectra were obtained in positive ion mode using electron spray ionization (ESI) technique. Compound 3 was purchased from TCI America.

3.1.1. 17-Oxosparteine (4)

To a stirred solution of (-)-sparteine (2.34 g, 10.0 mmol) in ethanol:water 1:1 (80 ml), 50 mL of 1 M aqueous KOH solution was added followed by potassium ferricyanide (16.4 g, 50.0 mmol). The reaction mixture was stirred for 1 h at room temperature. The aqueous layer was extracted with DCM (3 × 50 mL). The combined organic layers were dried with sodium sulfate and evaporated to dryness. The product was further purified using flash column chromatography on silica gel using diethyl ether as an eluent to give 4 (98%) as a white solid. ¹H NMR (400 MHz, CDCl₃) δ 0.82–1.39 (m, 13 H), 1.50–1.57 (m, 3 H), 1.67–1.70 (m, 1 H), 1.84–1.92 (m, 2 H), 2.08–2.14 (m, 1 H), 2.33–2.42 (m, 2 H), 2.84–2.87 (m, 1 H), 4.38–4.42 (m, 1 H). ¹³C NMR (100 MHz, CDCl₃) δ 23.7, 24.4, 24.5, 24.6, 26.3, 29.3, 32.6, 34.0, 41.3, 43.1, 55.8, 60.4, 62.1, 63.8, 168.5. HRMS (ESI): calcd for C₁₅H₂₅N₂O [M+H]⁺, 249.1966; found, 249.1961.

3.1.2. General procedure for compounds 5–10

Vaska's catalyst (1 mol%) and compound **4** (0.3 mmol, 1.0 eq) were charged into a dry 25 mL flask. Addition of dry DCM (3 mL) was followed by TMDS (0.6 mmol, 2.0 eq) while stirring at room temperature. The reaction mixture was stirred for 15 min, then cooled to -78°C . Grignard reagent (2.0 eq) was added dropwise. The solution was stirred at -78°C for 10 min, then warmed to room temperature and stirred for 4 h. The reaction mixture was quenched with saturated aqueous NH_4Cl solution and extracted with DCM (2×10 mL). The combined organic layers were dried over sodium sulfate, filtered and the solvent was removed under vacuum. The crude material was further purified by flash column chromatography using 5% methanol in DCM to furnish compounds **5–10**.

3.1.3. 17-Phenylsarteine (**5**)

Mp $101\text{--}103^{\circ}\text{C}$. Yield 61%. ^1H NMR (400 MHz, DMSO-d_6) δ 1.11–1.17 (m, 3 H), 1.37–1.59 (m, 9 H), 1.76–1.82 (m, 3 H), 1.93–1.96 (m, 1 H), 2.09–2.12 (m, 2 H), 2.31–2.33 (m, 2 H), 2.63–2.74 (m, 3 H), 3.32–3.35 (m, 2 H), 7.15–7.21 (m, 3 H), 7.38–7.41 (m, 2 H). ^{13}C NMR (100 MHz, DMSO-d_6) δ 25.9, 26.7, 26.8, 26.9, 28.4, 32.1, 35.1, 35.9, 44.2, 45.9, 58.1, 63.4, 65.1, 66.2, 73.1, 124.3, 125.2, 129.1, 139.8. HRMS (ESI): calcd for $\text{C}_{21}\text{H}_{31}\text{N}_2$ $[\text{M} + \text{H}]^+$, 311.2487; found, 311.2492.

3.1.4. 17-(4'-Methoxyphenyl)sarteine (**6**)

Mp $115\text{--}116^{\circ}\text{C}$. Yield 59%. ^1H NMR (400 MHz, DMSO-d_6) δ 1.15–1.23 (m, 3 H), 1.41–1.67 (m, 9 H), 1.78–1.86 (m, 3 H), 1.93–1.96 (m, 1 H), 2.05–2.10 (m, 2 H), 2.27–2.34 (m, 2 H), 2.59–2.69 (m, 3 H), 3.31–3.34 (m, 2 H), 3.68 (s, 3 H), 7.01 (d, $J = 7.6$ Hz, 2 H), 7.25 (d, $J = 7.6$ Hz, 2 H). ^{13}C NMR (100 MHz, DMSO-d_6) δ 24.9, 25.9, 26.1, 26.6, 27.8, 30.7, 33.5, 36.1, 44.2, 44.9, 56.1, 60.2, 61.8, 63.7, 64.9, 72.1, 111.6, 129.1, 139.6, 156.1. HRMS (ESI): calcd for $\text{C}_{22}\text{H}_{33}\text{N}_2\text{O}$ $[\text{M} + \text{H}]^+$, 341.2592; found, 341.2598.

3.1.5. 17-(3',4',5'-Trimethoxyphenyl)sarteine (**7**)

Mp $97\text{--}99^{\circ}\text{C}$. Yield 51%. ^1H NMR (400 MHz, DMSO-d_6) δ 1.10–1.18 (m, 3 H), 1.38–1.62 (m, 9 H), 1.75–1.83 (m, 3 H), 1.92–1.95 (m, 1 H), 2.08–2.13 (m, 2 H), 2.30–2.37 (m, 2 H), 2.63–2.75 (m, 3 H), 3.45–3.49 (m, 2 H), 3.75 (s, 3 H), 3.85 (s, 6 H), 7.25 (s, 2 H). ^{13}C NMR (100 MHz, DMSO-d_6) δ 25.7, 26.2, 26.4, 26.7, 28.1, 31.3, 34.3, 35.6, 43.1, 45.0, 57.5, 57.6, 61.6, 62.2, 64.0, 65.8, 70.2, 106.2, 133.2, 144.3, 154.8. HRMS (ESI): calcd for $\text{C}_{24}\text{H}_{37}\text{N}_2\text{O}_3$ $[\text{M} + \text{H}]^+$, 401.2804; found, 401.2801.

3.1.6. 17-(4'-Chlorophenyl)sarteine (**8**)

Mp $123\text{--}125^{\circ}\text{C}$. Yield 72%. ^1H NMR (400 MHz, DMSO-d_6) δ 1.08–1.14 (m, 3 H), 1.30–1.51 (m, 9 H), 1.71–1.76 (m, 3 H), 1.88–1.91 (m, 1 H), 2.01–2.06 (m, 2 H), 2.27–2.30 (m, 2 H), 2.59–2.65 (m, 3 H), 3.57–3.60 (m, 2 H), 7.89 (d, $J = 6.9$ Hz, 2 H), 7.97 (d, $J = 6.9$ Hz, 2 H). ^{13}C NMR (100 MHz, DMSO-d_6) δ 24.1, 25.8, 25.9, 26.0, 27.5, 30.6, 33.8, 35.0, 44.2, 45.5, 56.8, 63.1, 65.1, 65.9, 71.2, 127.9, 128.8, 139.1, 141.2. HRMS (ESI): calcd for $\text{C}_{21}\text{H}_{30}\text{ClN}_2$ $[\text{M} + \text{H}]^+$, 345.2097; found, 345.2092.

3.1.7. 17-(4'-Nitrophenyl)sarteine (**9**)

Mp $108\text{--}110^{\circ}\text{C}$. Yield 55%. ^1H NMR (400 MHz, DMSO-d_6) δ 1.11–1.17 (m, 3 H), 1.37–1.59 (m, 9 H), 1.76–1.82 (m, 3 H), 1.93–1.96 (m, 1 H), 2.09–2.12 (m, 2 H), 2.31–2.33 (m, 2 H), 2.63–2.74 (m, 3 H), 3.53–3.56 (m, 2 H), 8.16 (d, $J = 7.4$ Hz, 2 H), 8.40 (d, $J = 7.4$ Hz, 2 H). ^{13}C NMR (100 MHz, DMSO-d_6) δ 25.7, 26.2, 26.5, 26.7, 28.1, 31.3, 34.3, 35.6, 43.1, 45.0, 57.5, 62.2, 64.0, 65.8, 70.4, 125.7, 132.1, 141.5, 144.3. HRMS (ESI): calcd for $\text{C}_{21}\text{H}_{30}\text{N}_3\text{O}_2$ $[\text{M} + \text{H}]^+$, 356.2338; found, 356.2343.

3.1.8. 17-(4'-Quinoliny)sarteine (**10**)

Mp $137\text{--}139^{\circ}\text{C}$. Yield 68%. ^1H NMR (400 MHz, DMSO-d_6) δ 1.07–1.14 (m, 3 H), 1.34–1.60 (m, 9 H), 1.74–1.79 (m, 3 H), 1.91–1.94

(m, 1 H), 2.06–2.10 (m, 2 H), 2.28–2.35 (m, 2 H), 2.61–2.71 (m, 3 H), 3.52–3.56 (m, 2 H), 7.76–7.79 (m, 1 H), 7.85–7.88 (m, 1 H), 8.04 (d, $J = 4.5$ Hz, 1 H), 8.15 (d, $J = 8.1$ Hz, 1 H), 8.95–9.98 (m, 1 H), 9.23 (d, $J = 4.5$ Hz, 1 H). ^{13}C NMR (100 MHz, DMSO-d_6) δ 24.1, 24.7, 25.0, 25.1, 26.5, 29.7, 32.7, 34.0, 41.5, 43.5, 55.9, 60.6, 62.4, 64.2, 71.1, 123.2, 124.1, 125.8, 129.0, 129.5, 130.0, 136.3, 148.4, 151.1. HRMS (ESI): calcd for $\text{C}_{24}\text{H}_{32}\text{N}_3$ $[\text{M} + \text{H}]^+$, 362.2596; found, 362.2599.

3.2. Antiproliferative activity

The *in vitro* cytotoxicity testing of compounds **5–10** was performed against four cancer cell lines and mouse embryo fibroblast cells adopting MTT assay as previously described after 48 h treatment with the tested compounds (Mosmann, 1983).

3.3. Autophagic protein degradation assay

The effect of **10** (10 mM) on the degradation of [^{14}C]-valine-labeled long-lived proteins in HeLa cells was performed as previously described (Dupont et al., 2017) using NH_4Cl as a negative control and 3-methyladenine (10 mM) as positive control.

3.4. Intracellular ATP assay

The intracellular ATP level in HeLa cells was determined using ATP assay kit purchased from abcam (ab83355). The assay was performed according to the protocol provided.

4. Conclusion

In a summary, arylsarteine derivatives were synthesized and evaluated for their antiproliferative activity. Incorporation of electron withdrawing groups (EWGs) to the aryl substituents enhanced the antiproliferative activity of the arylsarteine derivatives. Compound **10** bearing 4-quinoliny moiety as the aryl substituent demonstrated promising antiproliferative activity against A549 and HeLa cancer cell lines. The antiproliferative activity of **10** is directly related to the blockade of autophagic flux in cancer cells as revealed by monitoring autophagic protein degradation and intracellular ATP level in HeLa cells.

Appendix A. Supplementary data

Supplementary material related to this article can be found, in the online version, at doi:<https://doi.org/10.1016/j.phytol.2018.07.022>.

References

- Amaravadi, R.K., Yu, D., Lum, J.J., Bui, T., Christophorou, M.A., Evan, G.I., et al., 2007. Autophagy inhibition enhances therapy-induced apoptosis in a Myc-induced model of lymphoma. *J. Clin. Invest.* 117, 326–336.
- Anding, A.L., Baehrecke, 2015. Autophagy in cell life and cell death. *Curr. Top. Dev. Biol.* 114, 67–91.
- Bao, Y., Kong, X., Yang, L., Liu, R., Shi, Z., Li, W., Hua, B., Hou, W., 2014. Complementary and alternative medicine for cancer pain: an overview of systematic reviews. *Evid. Complement. Alternat. Med.* 2014, 170396.
- Bi, C., Zhang, C., Li, Y., Tang, S., Deng, H., Zhao, W., Wang, Z., Shao, R., Song, D., 2014. Novel N-substituted sophoridinol derivatives as anticancer agents. *Eur. J. Med. Chem.* 81, 95–105.
- Bi, C., Ye, C., Li, Y., Zhao, W., Shao, R., Song, D., 2016. Synthesis and biological evaluation of 12-N-p-chlorobenzyl sophoridinol derivatives as a novel family of anticancer agents. *Acta Pharm. Sin.* 37, 222–228.
- Bi, C., Zhang, N., Yang, P., Ye, C., Wang, Y., Fan, T., Shao, R., Deng, H., Song, D., 2017. Synthesis, biological evaluation, and autophagy mechanism of 12N-substituted sophoridinamines as novel anticancer agents. *ACS Med. Chem. Lett.* 8, 245–250.
- Carew, J.S., Nawrocki, S.T., Cleveland, J.L., 2007. Modulating autophagy for therapeutic benefit. *Autophagy* 3, 464–467.
- Dupont, N., Leroy, C., Hamai, A., Codogno, P., 2017. Long-lived protein degradation during autophagy. *Methods Enzymol.* 588, 31–40.
- Galluzzi, L., Pietrocola, F., Levine, B., et al., 2014. Metabolic control of autophagy. *Cell* 159, 1263–1276.

- Garcia-Lopez, P.M., de la Mora, P.G., Wysocka, W., Maiztegui, B., Alzugaray, M.E., Del Zotto, H., et al., 2004. Quinolizidine alkaloids isolated from *Lupinus* species enhance insulin secretion. *Eur. J. Pharmacol.* 504, 139–142.
- Golden, E.B., Cho, H., Hofman, F.M., Louie, S.G., Schonthal, A.H., Chen, T.C., 2015. Quinoline-based antimalarial drugs: a novel class of autophagy inhibitors. *Neurosurg. Focus* 38, E12.
- Golebiewski, W.M., Spenser, I.D., 1985. Lactams of sparteine. *Can. J. Chem.* 63, 716–719.
- Guo, Y.M., Huang, Y.X., Shen, H.H., Sang, X.X., Ma, X., Zhao, Y.L., Xiao, X.H., 2015. Efficacy of compound kushen injection in relieving cancer-related pain: a systematic review and meta-analysis. *Evid. Complement. Alternat. Med.* 2015, 840742.
- Hatzold, T., Elmadfa, I., Gross, R., Wink, M., Hartmann, T., Witte, L., 1983. Quinolizidine alkaloids in seeds of *Lupinus mutabilis*. *J. Agric. Food Chem.* 31, 934–938.
- Khazir, J., Mir, B.A., Pilcher, L., Riley, D.L., 2014. Role of plants in anticancer drug discovery. *Phytochem. Lett.* 7, 173–181.
- Mizushima, N., Komatsu, M., 2011. Autophagy: renovation of cells and tissues. *Cell* 147, 728–741.
- Mosmann, T., 1983. Rapid colorimetric assay for cellular growth and survival: application to proliferation and cytotoxicity assays. *J. Immunol. Methods* 65, 55–63.
- Pugsley, M.K., Saint, D.A., Hayes, E., Berlin, K.D., Walker, M.J., 1995. The cardiac electrophysiological effects of sparteine and its analogue BRB-I-28 in the rat. *Eur. J. Pharmacol.* 294, 319–327.
- Sun, M., Cao, H., Sun, L., Dong, S., Bian, Y., Han, J., Zhang, L., Ren, S., Hu, Y., Liu, C., Xu, L., Liu, P., 2012. Antitumor activities of kushen: literature review. *Evid. Complement. Alternat. Med.* 2012, 373219.
- Wang, L., You, Y., Wang, S., Liu, X., Liu, B., Wang, J., Lin, X., Chen, M., Liang, G., Yang, H., 2012. Synthesis, characterization and in vitro anti-tumor activities of matrine derivatives. *Bioorg. Med. Chem. Lett.* 22, 4100–4102.
- Wang, Y.X., Liu, Z.D., Bi, C.W., Liu, L., Deng, H.B., Song, D.Q., 2017. How can tricyclic sophoridinic derivatives be used as autophagy inhibitors for cancer treatments? *Future Med. Chem.* 9, 835–837.
- Wei, Y., Wu, X., Liu, X., Luo, J., 2006. A rapid reversed phase high performance liquid chromatographic method for determination of sophoridine in rat plasma and its application to pharmacokinetics studies. *J. Chromatogr. B: Anal. Technol. Biomed. Life Sci.* 843, 10–14.
- Xu, W., Lin, H., Zhang, Y., Chen, X., Hua, B., Hou, W., Qi, X., Pei, Y., Zhu, X., Zhao, Z., Yang, L., 2011. Compound kushen injection suppresses human breast cancer stem-like cells by down-regulating the canonical Wnt/beta-catenin pathway. *J. Exp. Clin. Cancer Res.* 30, 103.
- Xu, Z., Zhanf, F., Bai, C., Yao, C., Zhong, H., Zou, C., Chen, X., 2017. Sophoridine induces apoptosis and S phase arrest via ROS-dependent JNK and ERK activation in human pancreatic cancer cells. *J. Exp. Clin. Cancer Res.* 36, 124.
- Yang, J., Zhu, L., Wu, Z., Wang, Y., 2013. Chinese herbal medicines for induction of remission in advanced or late gastric cancer. *Cochrane Database Syst. Rev.* 4, CD005096.
- Zhao, Z., Fan, H., Higgins, T., Qi, J., Haines, D., Trivett, A., Oppenheim, J.J., Wei, H., Li, J., Lin, H., Howard, O.M., 2014. Fufang Kushen injection inhibits sarcoma growth and tumor-induced hyperalgesia via TRPV1 signaling pathways. *Cancer Lett.* 355, 232–241.
- Zhao, L., Mao, L., Hong, G., Yang, X., Liu, T., 2015. Design, synthesis and anticancer activity of matrine-1*H*-1,2,3-triazole-chalcone conjugates. *Bioorg. Med. Chem. Lett.* 25, 2540–2544.